THE EFFECTS OF BINARITY ON PLANET OCCURRENCE RATES MEASURED BY TRANSIT SURVEYS

L. G. BOUMA,[1] K. MASUDA,[1] AND J. N. WINN[1]

[1]*Department of Astrophysical Sciences, Princeton University, 4 Ivy Lane, Princeton, NJ 08540, USA*

ABSTRACT

Wide-field surveys for transiting planets, such as the NASA *Kepler* and *TESS* missions, are usually conducted without knowing which stars are binaries. Unresolved and unrecognized binary stars give rise to systematic errors in planet occurrence rates, including misclassified planets and miscounts in the number of searched stars. The individual errors can have different signs, making it difficult to anticipate the net effect on inferred occurrence rates. Here we use simplified models of signal-to-noise limited transit surveys to try and clarify the situation. We derive a formula for the apparent occurrence rate density measured by an observer who falsely assumes all stars are single. The formula depends on the binary fraction; the mass function of the secondary stars; and the true occurrence of planets around primaries, secondaries, and single stars. It also takes into account the Malmquist bias by which binaries are over-represented in flux-limited samples. Application of the formula to an idealized *Kepler*-like survey shows that for planets larger than $2r_\oplus$, the net systematic error is of order 10%. One consequence is that unrecognized binaries cannot account for the apparent discrepancy between hot Jupiter occurrence rates measured by transit and RV surveys. For smaller planets the errors are potentially larger: the occurrence of Earth-sized planets could be overestimated by as much as a factor of two. We also show that if high-resolution imaging reveals a transit host star to be a binary, the planet is usually more likely to orbit the primary star than the secondary star.

Keywords: methods: data analysis — planets and satellites: detection — surveys

Corresponding author: L. Bouma
luke@astro.princeton.edu

1. INTRODUCTION

One of the goals of exoplanetary science is to establish how common, or rare, are planets of various types. Knowledge of planet occurrence rates is helpful for inspiring and testing theories of planet formation, designing the next generation of planet-finding surveys, and simply satisfying our curiosity about other worlds. One method for measuring occurrence rates is to monitor the brightnesses of many stars over a wide field, seeking evidence for planetary transits. Measuring occurrence rates using this method was the highest priority of the NASA *Kepler* mission. Great strides have been made in the analysis of *Kepler* data, including progress towards measuring the fraction of Sun-like stars that harbor Earth-like planets (Youdin 2011; Petigura et al. 2013; Dong & Zhu 2013; Foreman-Mackey et al. 2014; Burke et al. 2015)

A lingering concern in occurrence rate studies is that in most cases, investigators have assumed that all of the sources of light that were monitored are single stars (*e.g.*, Howard et al. 2012; Fressin et al. 2013; Dressing & Charbonneau 2015; Burke et al. 2015). In reality, many of the point sources seen in a transit survey are unresolved multiple-star systems, especially binaries. Unrecognized binaries cause numerous systematic errors in the planetary occurrence rates. For example, when there is a transiting planet around a star in a binary, the additive constant light from the second star reduces the fractional loss of light due to the planet. This makes transit signals harder to detect and lowers the number of detections. On the other hand, in a binary there are two opportunities to detect transiting planets, which could increase the overall number of detections.

At the outset of this study it was not clear to us whether the neglect of binaries was a serious issue at all, or even whether the net effect of all the errors is positive or negative. The goals of this study were to provide a framework for dealing with these issues, and to calculate a leading-order estimate for the net systematic effects. In this spirit, our models are idealized and analytic, and we do not attempt a detailed correction of the results from *Kepler* or any other real transit survey.

This paper is organized as follows. The next section enumerates the various errors that arise from unrecognized binaries. Then in Section 3, we develop an idealized model of a transit survey in which all planets have identical properties, and all stars are identical except that some fraction are in binary systems. This simple model motivates the derivation of a general formula, given in Section 4, that allows for more realistic stellar and planetary populations. We use this formula in Section 5 to explore more complicated but nevertheless still analytic models. In Section 6 we discuss the errors due to unrecognized binaries for specific cases of current interest: the occurrence of Earth-like planets; the apparent discrepancy between hot Jupiter occurrence rates in different surveys; and the shape of the "evaporation valley" in the planet radius distribution that was brought to light by Fulton et al. (2017). We review all the results in Section 7.

2. UNDERSTANDING THE ERRORS

Imagine a group of astronomers that wants to measure the mean number of planets of a certain type per star of a certain type. They perform a wide-field photometric search for planets that transit, and discover all for which

$$\frac{\delta}{\sigma} > \left(\frac{S}{N}\right)_{\min}. \tag{1}$$

Here the signal S is the observed transit depth δ, in units of relative flux. The noise N is the uncertainty in the determination of the flux ratio of the star inside and outside of transits. The minimum signal-to-noise for detection, $(S/N)_{\min}$, depends on the properties of the telescope. We will assume throughout this paper that the photometric uncertainty scales as the inverse square root of the number of photons collected from the source, *i.e.*, the dependence on stellar properties is $\sigma \propto (L_{\rm tot}/d^2)^{-1/2}$, where $L_{\rm tot}$ is the total luminosity of the stellar system and d is its distance from Earth. The observed signal amplitude δ depends on the fraction of the total luminosity that comes from the planet-hosting star, since light from unresolved stellar companions is not affected by the planet's transit.

The astronomers analyze their data assuming that all stars are single. In particular they do not have accurate enough parallaxes to tell that some of the stars are apparently overluminous. They want to compute the number of planets with size r per star of mass M. If the total number of stars for which such planets could be detected ($N_\star$) and the number of detected planets ($N_{\rm det}$) are both large, then the astronomers' estimate for the occurrence rate (Λ) is simply

$$\Lambda = \frac{N_{\rm det}}{N_\star} \times \frac{1}{p_{\rm tra}}, \tag{2}$$

where the geometric transit probability, $p_{\rm tra}$, accounts for the fact that most planetary orbits are not aligned close enough with our line of sight to produce transits.

There are many potential pitfalls in this calculation. Some genuine transit signals are missed even if they formally exceed the signal-to-noise threshold, because of the probabilistic nature of transit detection. Planets can be misclassified due to statistical and systematic errors in the catalogued properties of the stars. Some apparent transit signals are spurious, arising from noise fluctuations or failures of "detrending" the astrophysical or instrumental variations in the photometric signal. Poor angular resolution leads to blends between eclipsing binary stars and other stars along nearly the same line of sight, producing signals that mimic those of transiting planets.

We will focus exclusively on problems that arise from the fact that many stars exist in gravitationally bound binary systems. Even with this narrow focus, there are numerous sources of error. All three of the quantities in Equation 2 are subject to observational bias:

1. The detected planet count, $N_{\rm det}$, is actually the number of detected planets that *appear* to have size r, orbiting stars that *appear* to have mass M. Whenever the planet-hosting star is part of a binary,

   - the planet's size will be misclassified because of the reduction in the amplitude of the photometric signal;
   - the host star's properties could be misclassified because its light is combined with a second star of a different spectral type.

2. The apparent number of stars that were searched, $N_\star$, is biased

   - toward lower values, because it does not include all of the secondary stars that were searched for transiting planets;
   - toward higher values, because some of the stars that appeared to be suitably small and bright to detect the desired type of planet are in fact binaries for which the amplitude of the photometric signal would be reduced to an undetectable level.

3. The transit probability $p_{\rm tra}$, which scales with the stellar mean density as $\rho^{-1/3}$, is biased because the planet-hosting star could be misclassified.

Two other problems that may arise are not represented in Equation 2. One is astrophysical: the true occurrence rate of the desired type of planet may depend on whether the host is a single star, the primary star of a binary, or the secondary star of a binary. Such differences could be caused by the requirement for long-term dynamical stability, or differences in the planet formation process. When the search sample includes both singles and binaries, the detected planets are thereby drawn from different occurrence distributions (see Wang et al. 2015a; Kraus et al. 2016).

The other problem is an observational effect. In the searched sample, the ratio between the number of binary and single stars will differ from that in a volume-limited sample due to a type of Malmquist bias. The total luminosity of a binary is larger than the luminosity of either the primary or secondary star. This means that for transit signals of a given amplitude, the binaries are searchable at greater distances from the Earth. Thus for any planet and star pair, adding a stellar companion both helps and hinders transit detection: the extra photons help by lowering the noise, and hinder by diminishing the observed transit depth.

Planet occurrence rates are often presented as two-dimensional density functions in the space of planet radius and orbital period. Thankfully none of the errors we have enumerated lead to errors in the period distribution. When more than one transit is detected (as is usually required by the surveyors), the orbital periods can be measured without ambiguity regardless of whether the host star is single or one member of a binary. Hence in what follows, we focus on the radius distribution and assume the periods are measured without significant uncertainty.
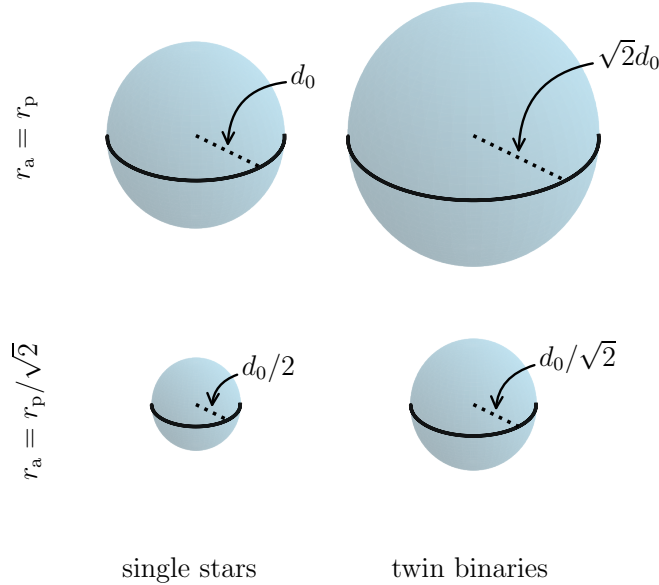
Figure 1. Searchable volumes for single stars (*left*) and twin binaries (*right*), assuming that all stars have the same mass, radius, and luminosity, and that all planets have the same radius r_p. *Top:* At an apparent radius $r_\mathrm{a} = r_\mathrm{p}$, the binarity-ignoring observers search twin binaries out to a distance $\sqrt{2}$ times greater than they search single stars. Because the transit depths are diluted, there are no planets in twin binaries with $r_\mathrm{a} = r_\mathrm{p}$. *Bottom:* At $r_\mathrm{a} = r_\mathrm{p}/\sqrt{2}$, the observed transit depths are smaller by a factor of two, so the maximum searchable distances are half those at $r_\mathrm{a} = r_\mathrm{p}$. The only detected planets with $r_\mathrm{a} = r_\mathrm{p}/\sqrt{2}$ orbit twin binaries.

Given all of the confusing and opposing sources of error, we will proceed in stages. We start from a barebones model in which everything can be written down on the back of a napkin, and build up to an analytic model allowing for generality in the distribution of the binaries and the planets they host.

3. SIMPLE MODELS

3.1. *One type of star, one type of planet*

Since the effects of binarity are most pronounced when the two stellar components are similar, we begin by considering a universe in which all stars are identical, with mass M, radius R, and luminosity L. Some fraction of them exist in twin binaries. All planets have size r_p. In this scenario, stellar radii are never misclassified because the combined light of a binary has the same color and spectrum as a single star. We further assume that planets occur around single stars and members of binaries at the same rate, $\Lambda(r_\mathrm{p})$.

Our naive observers detect transiting planets with two different depths. Since

$$\delta = \left(\frac{r_\mathrm{p}}{R}\right)^2 \frac{L}{L_\mathrm{tot}}, \tag{3}$$

one class of transit signal, with depth $(r_{\mathrm{p}}/R)^2$, occurs in single star systems. The other class, with half the depth, occurs in twin binary systems, leading to apparent planet radii $\sqrt{2}$ smaller than the true radii.

To calculate the occurrence rate of each planet type, our observers identify the "stars" from their survey that appear to have been searched for signals of each depth. These transits are detected within a certain maximum distance (see Pepper et al. 2003; Pepper & Gaudi 2005), which from Equation 1 scales as

$$d_{\max} \propto \delta \cdot L_{\mathrm{tot}}^{1/2}. \tag{4}$$

Assuming that stars are uniformly distributed in space, the number of searchable stars $N_\star$ is proportional to

$$N_\star \propto n\delta^3 L_{\mathrm{tot}}^{3/2}, \tag{5}$$

where n is the number per unit volume of single or binary star systems.

When selecting sources that appear to have been searched, the observers admit some binaries. Since the binaries are twice as luminous as singles, at fixed δ they are included out to a distance that is larger by a factor of $\sqrt{2}$. To detect the half-strength signal, the observers need the noise level to be lower by a factor of two, which means the flux must be four times higher than that of a single star at distance d_0. This is true of single stars within a distance $d_0/2$, and binaries within a distance $d_0\sqrt{2}/2$. The searchable volumes are illustrated in Figure 1.

Putting it all together, the *apparent* occurrence rate Λ_{a} of planets of radius r_{p} will be

$$\Lambda_{\mathrm{a}}(r_{\mathrm{p}}) = \frac{\Lambda(r_{\mathrm{p}})\, n_{\mathrm{s}} d_0^3}{n_{\mathrm{s}} d_0^3 + n_{\mathrm{b}}(d_0\sqrt{2})^3} \tag{6}$$

where n_{s} and n_{b} are the number densities of single and binary star systems, respectively. This apparent rate is larger than the true rate by a factor

$$\frac{\Lambda_{\mathrm{a}}(r_{\mathrm{p}})}{\Lambda(r_{\mathrm{p}})} = \frac{1}{1 + 2^{3/2}(n_{\mathrm{b}}/n_{\mathrm{s}})}. \tag{7}$$

The observers will also claim to have discovered a class of planet with radius $r_{\mathrm{p}}/\sqrt{2}$ and an occurrence rate given by

$$\frac{\Lambda_{\mathrm{a}}(r_{\mathrm{p}}/\sqrt{2})}{\Lambda(r_{\mathrm{p}})} = \frac{2n_{\mathrm{b}}(d_0\sqrt{2}/2)^3}{n_{\mathrm{s}}(d_0/2)^3 + n_{\mathrm{b}}(d_0\sqrt{2}/2)^3} = \frac{2 \cdot 2^{3/2}(n_{\mathrm{b}}/n_{\mathrm{s}})}{1 + 2^{3/2}(n_{\mathrm{b}}/n_{\mathrm{s}})}. \tag{8}$$

We can now assess the severity of these errors, given the binary-to-single ratio $n_{\mathrm{b}}/n_{\mathrm{s}}$. For stars with masses from 0.7 to 1.3 $M_\odot$, Raghavan et al. (2010) found the multiplicity fraction – the fraction of systems in a volume-limited sample that are multiple – to be 0.44. Assuming all multiple systems are binaries, this means

$$\frac{n_{\mathrm{b}}}{n_{\mathrm{s}} + n_{\mathrm{b}}} \approx 0.44. \tag{9}$$
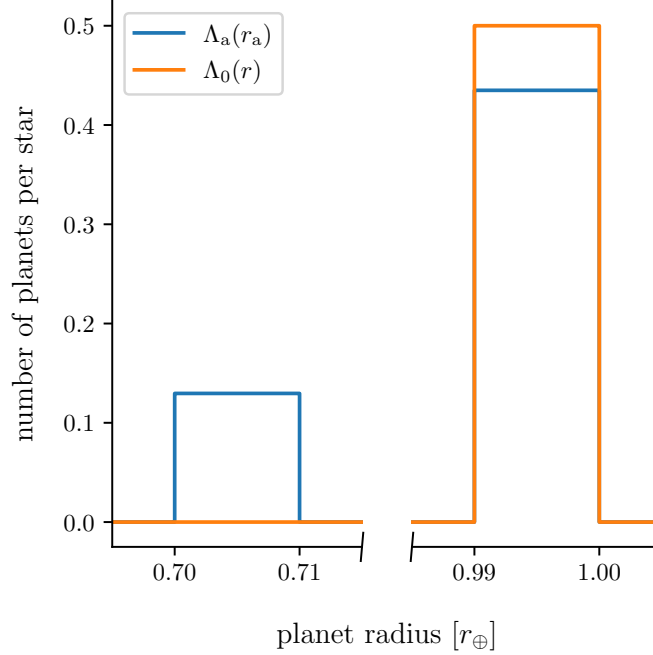
Figure 2. Apparent occurrence rate Λ_a, and occurrence rate for singles Λ_0, for a model with one type of star, one type of planet, and twin binaries (same as Figure 1). We assume a twin binary fraction of 0.05, and that single, primary, and secondary stars host planets at equal rates. If the true planet radius is r_p, all planets detected in binaries will have apparent radii $r_a = r_p/\sqrt{2}$; Equation 10 gives the normalizations.

Of course not all of these binaries are "twin" binaries as we have assumed in our simple calculation. Perhaps only a tenth of the binaries have pairs of stars close enough in their basic properties to produce errors as significant as those we have been considering. In detail, this fraction depends on the binary mass ratio distribution and stellar mass-luminosity relation (see Section 4). Taking a leading-order estimate of $n_b/(n_s + n_b) \approx 0.05$, we find

$$\frac{\Lambda_a(r_p)}{\Lambda(r_p)} = 0.87, \quad \frac{\Lambda_a(r_p/\sqrt{2})}{\Lambda(r_p)} = 0.26. \tag{10}$$

All together, the various effects produce biases of order 10% in the occurrence rates. We will see that this level of error is characteristic of many of our more complicated models as well.

3.2. *Formula Based on Apparent Rate Density*

There is a different way to conceptualize the preceding results that will be useful in the upcoming discussion. We now consider a spectrum of planet sizes, r, and introduce the occurrence rate density

$$\Gamma(r) \equiv \frac{d\Lambda}{dr}, \tag{11}$$

the number of planets per star per unit planet radius.

The naive observers are in fact measuring $\Gamma_{\rm a}(r_{\rm a})$, the *apparent* occurrence rate density – the number of planets per star per unit apparent radius $r_{\rm a}$. The "apparent planet radius" is the radius inferred from the transit depth under the assumption that the host star is single. The "apparent stellar radius" $R_{\rm a}$ is analogous. The observed transit depth can be written $\delta = (r_{\rm a}/R_{\rm a})^2$, which from Equation 3 gives $r_{\rm a} = r_{\rm p}/\sqrt{2}$ for planets in twin binaries. $\Gamma_{\rm a}(r_{\rm a})$ is the same as the *true* rate density of transit signals of amplitude δ.

We will now calculate the apparent rate density by evaluating the star and planet counts for signals coming from single stars, primary stars in binaries, and secondary stars in binaries. Let μ be the ratio between the number of searchable binary systems and the number of searchable single systems at a particular transit depth. The number of single and binary sources in the searched sample are then

$$\frac{N_\star(r_{\rm a})}{1+\mu} \quad \text{and} \quad \frac{\mu N_\star(r_{\rm a})}{1+\mu}, \tag{12}$$

respectively. Earlier we showed that due to Malmquist bias, $\mu = 2^{3/2}(n_{\rm b}/n_{\rm s})$.

Suppose the occurrence rate densities for planets around single stars, primaries, and secondaries are $\Gamma_0(r), \Gamma_1(r)$, and $\Gamma_2(r)$, respectively. For a single planet size,

$$\Gamma_i(r) = \Lambda(r_{\rm p}) \cdot \hat{\delta}(r - r_{\rm p}), \quad \text{for } i \in \{0, 1, 2\}, \tag{13}$$

where $\hat{\delta}$ is the Dirac delta function. The number of planets detected from singles, primaries, and secondaries are then

$$n_{\rm det}^0(r_{\rm a}){\rm d}r_{\rm a} = \frac{N_\star(r_{\rm a})}{1+\mu}p_{\rm tra}\Gamma_0(r_{\rm a}){\rm d}r_{\rm a}, \tag{14}$$

$$n_{\rm det}^1(r_{\rm a}){\rm d}r_{\rm a} = \frac{\mu N_\star(r_{\rm a})}{1+\mu}p_{\rm tra}\Gamma_1(\sqrt{2}r_{\rm a}){\rm d}(\sqrt{2}r_{\rm a}), \tag{15}$$

$$n_{\rm det}^2(r_{\rm a}){\rm d}r_{\rm a} = \frac{\mu N_\star(r_{\rm a})}{1+\mu}p_{\rm tra}\Gamma_2(\sqrt{2}r_{\rm a}){\rm d}(\sqrt{2}r_{\rm a}), \tag{16}$$

where $n_{\rm det}^i$ is the number of detections per unit apparent radius for each respective type of star.

Dividing the number of detections by the number of sources, the apparent rate density reported when ignoring binarity is

$$\Gamma_{\rm a}(r_{\rm a}) = \frac{1}{1+\mu}\Gamma_0(r_{\rm a}) + \frac{\mu}{1+\mu}\sqrt{2}\,\Gamma_1(\sqrt{2}r_{\rm a}) + \frac{\mu}{1+\mu}\sqrt{2}\,\Gamma_2(\sqrt{2}r_{\rm a}). \tag{17}$$

If we insert Equation 13 and integrate over apparent radius, this reproduces Equations 6 and 8.

4. GENERAL FORMULA FOR APPARENT OCCURRENCE RATE

To generalize the procedure of Section 3.2 for binaries with varying light ratios, we consider an SNR-limited survey in which stars can have arbitrary properties.

We assume that there are some functions $L(M)$ and $R(M)$ that specify a star's luminosity and radius in terms of its mass. We also presume that the observers know the masses of every single and primary star, and that they assign each binary system the properties of its primary. Finally, we take the volume-limited distribution of binary mass ratios, $f(q)$, to be independent of the primary star's mass.

We want an equation for $\Gamma_a(r_a, M_a)$, the apparent rate density at each apparent planet radius and apparent stellar mass[1]. Similar to Equation 11, we define $\Gamma(r, M)$ as the number of planets per star, per unit planet radius, per unit stellar mass. Due to the varying binary mass ratios, we need the following modifications to Equation 17:

1. The Malmquist bias is different. The ratio between the number of binary and single systems for which a transit of depth δ is detectable, μ, has changed. At any (r_a, M_a) pair, the number of binary systems in the searchable volume with mass ratio $(q, q + dq)$ is now

$$\frac{N_\star(r_a)}{1 + \mu} \times \frac{n_b}{n_s} \left[\frac{L_{tot}(M_a, q)}{L(M_a)} \right]^{3/2} f(q)\, dq, \qquad (18)$$

where μ is given by

$$\mu = \int_0^1 \frac{n_b}{n_s} \left[\frac{L_{tot}(M_a, q)}{L(M_a)} \right]^{3/2} f(q)\, dq. \qquad (19)$$

Binaries with larger mass ratios are overrepresented by a factor of $[L_{tot}(M_a, q)/L(M_a)]^{3/2}$ because the sample of searchable binaries is magnitude-limited. To obtain the number of binary systems searched at each (r_a, M_a) pair, Equation 18 needs to be integrated over q. It can then replace $\mu N_\star(r_a)/(1 + \mu)$ in Equations 15 and 16.

2. The apparent radius of a planet in a binary system now depends on whether the host star is the primary or the secondary. When the host is the primary, we write $r = \mathcal{D}_1 r_a$, where

$$\mathcal{D}_1 = \left(\frac{L_{tot}(M_a, q)}{L(M_a)} \right)^{1/2}. \qquad (20)$$

When the host is the secondary, $r = \mathcal{D}_2 r_a$, and the ratio between the assumed and true stellar radii must be included:

$$\mathcal{D}_2 = \frac{R(qM_a)}{R(M_a)} \left(\frac{L_{tot}(M_a, q)}{L(qM_a)} \right)^{1/2}. \qquad (21)$$

3. Since the observers assign binaries the properties of the primary, the transit probability for planets orbiting secondaries is over-estimated. At a fixed orbital period, this changes p_{tra} in Equation 16 by a factor of

$$\frac{R(qM_a)}{R(M_a)} q^{-1/3}. \qquad (22)$$

---

[1] By assumption, the apparent stellar mass for single star systems is the true mass. For binary systems, the apparent mass is the mass of the primary.

Taking these modifications into account, a general formula for the apparent rate density follows:

$$\Gamma_a(r_a, M_a) = \frac{1}{1+\mu} \cdot \left\{ \Gamma_0(r_a, M_a) + \frac{n_b}{n_s} \left[\int_0^1 dq\, \mathcal{D}_1^3 f(q) \cdot \mathcal{D}_1 \Gamma_1(\mathcal{D}_1 r_a, M_a) \right. \right.$$
$$\left. \left. + \int_0^1 dq\, \mathcal{D}_1^3 f(q) \cdot q \mathcal{D}_2 \Gamma_2(\mathcal{D}_2 r_a, q M_a) \cdot \frac{R(q M_a)}{R(M_a)} q^{-1/3} \right] \right\}. \quad (23)$$

We give an alternative derivation in the Appendix. With the definition of μ in Equation 19, Equation 23 can also be expressed as

$$\Gamma_a(r_a, M_a) = \frac{1}{1+\mu} \cdot \left[\Gamma_0(r_a, M_a) \right.$$
$$\left. +\mu \cdot \left\langle \mathcal{D}_1 \cdot \Gamma_1\left(\mathcal{D}_1 r_a, M_a\right) + q \mathcal{D}_2 \cdot \Gamma_2\left(\mathcal{D}_2 r_a, q M_a\right) \cdot \frac{R(q M_a)}{R(M_a)} q^{-1/3} \right\rangle \right], \quad (24)$$

where the angle brackets denote averaging over $\mathcal{D}_1^3 f(q)$. Summarized, the apparent rate density is a weighted sum of the rate densities from singles, primaries, and secondaries. The weights are determined by the fraction μ and mass ratio distribution $\mathcal{D}_1^3 f(q)$ of binaries *in the searchable volume*. The fraction μ gives the relative contributions from singles and binaries, and $\mathcal{D}_1^3 f(q)$ applies a Malmquist bias for binaries that are brighter. A final correction for secondaries accounts for the overestimated transit probability.

5. REALISTIC STAR AND PLANET DISTRIBUTIONS

We will now apply our general equation for the apparent rate density (Equation 23) to study the impact of unrecognized binaries in regimes of observational interest. In the following, we write the rate density for each type of star, $\Gamma_i(r)$, as the product of a shape function, normalized to unity, and a constant:

$$\Gamma_i(r) = Z_i f_i(r), \quad \text{for } i \in \{0, 1, 2\}, \quad (25)$$

where the respective indices correspond to single stars, primaries of binaries, and secondaries of binaries. The normalizations Z_i are each system type's occurrence rate Λ_i, integrated over all planetary radii. In other words, they are number of planets per single, primary, or secondary star. Our main interest is in varying the radius shape function and the relative values of the integrated occurrence rates. We will also briefly mention shape functions in stellar mass. For analytic simplicity, we will assume throughout this section that stars are a one-parameter family, given by $L \propto M^\alpha \propto R^\alpha$. Applying these power laws to Equations 20 and 21, we find

$$\mathcal{D}_1 = (1 + q^\alpha)^{1/2} \quad \text{and} \quad \mathcal{D}_2 = q(1 + q^{-\alpha})^{1/2} \quad (26)$$

for the radius dilution prefactors.

5.1. *Power law planet radius distribution*
5.1.1. *Twin binaries*

As a first step, we return to the case where all binaries are twins. However, we now let the planet radius distribution be a power law,

$$\Gamma_i(r) = Z_i f(r) = Z_i r^\gamma / \mathcal{N}_r, \tag{27}$$

for $\mathcal{N}_r$ the shape function's normalization. Applying Equation 23 gives the resulting apparent rate density,

$$\Gamma_a(r_a) = \frac{r_a^\gamma}{\mathcal{N}_r} \left[\frac{Z_0}{1+\mu} + 2^{\frac{\gamma+1}{2}} \frac{\mu}{1+\mu} (Z_1 + Z_2) \right]. \tag{28}$$

Under these assumptions, twin binaries simply shift the apparent radius distribution: $\Gamma_a(r_a) \propto r_a^\gamma$. As in Section 3.1, $\mu = 2^{3/2} n_b/n_s$. If planet occurrence is independent of system multiplicity, the "correction factor" relative to the rate density for singles is

$$\frac{\Gamma_a(r_a)|_{r_a=r}}{\Gamma_0(r)} = \frac{1 + 2^{\frac{\gamma+3}{2}}\mu}{1+\mu}. \tag{29}$$

For a binary fraction of 0.1, $\mu \approx 0.15$. Taking $\gamma = -2.92$ from Howard et al. (2012), we find that the apparent rate density is a mere 0.4% larger than the rate density of single stars. Fortuitously, the exponent of the radius distribution is close to -3, and the errors from neglecting binaries almost entirely cancel out.

The above estimate cannot apply at small radii, since the shape function diverges. Howard et al. (2012)'s results indicate that a single power law fits the planet radius distribution for radii greater than $2r_\oplus$. Similarly, there should be an upper radius limit, r_u, to the radius distribution, perhaps around $24r_\oplus$ based on the most inflated hot Jupiters. Imposing an upper cut-off of r_u would lead to smaller values of the apparent rate density down to $r_u/\sqrt{2}$, compared to a power law without the cut-off. We are not particularly interested in this effect because hot Jupiter occurrence rates are poorly described by a power law (see Section 5.3). All told, if our assumptions are applicable to real transit surveys, Equation 29 suggests that for apparent radii from $2r_\oplus$ to $17r_\oplus$, unrecognized binaries are a minor source of systematic error.

5.1.2. *Binaries with power law mass ratio distribution*

To check whether non-twin binaries change the preceding result, we now consider a distribution of binary mass ratios. Specifically, we take $f(q) = q^\beta / \mathcal{N}_q$, for $\mathcal{N}_q$ the normalization. This changes μ from the twin binary case; Equation 19 simplifies to

$$\mu = \frac{n_b}{n_s} \frac{1}{1+\beta} \int_0^1 (1+q^\alpha)^{3/2} q^\beta \, dq. \tag{30}$$

For the $\beta = 0$ case, this equation means there will be more twin-like binaries than faint binaries in the sample of stars that are searched at any transit depth (Figure 3).
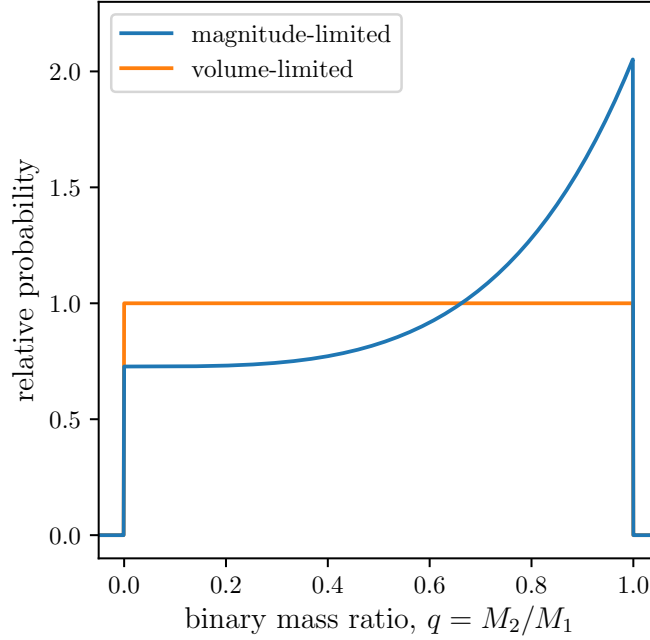
Figure 3. The mass ratio distribution for a magnitude-limited sample of binary stars, in which the underlying volume-limited distribution is uniform, qualitatively similar to Figure 16 of Raghavan et al. (2010). At a given observed transit depth, the searchable binaries in a transit survey are magnitude-limited. For this figure, we assume $L \propto M^{3.5}$.

The rate density now varies not only with planet radius, but also host star mass. We can absorb this dependence into a power law,

$$\Gamma_i(r, M) = Z_i \times \frac{r^\gamma}{\mathcal{N}_r} \times \frac{M^\zeta}{\mathcal{N}_M}, \tag{31}$$

where Z_i is dimensionless, and the normalization constants carry the units.

Our main interest is in the apparent rate density's radius dependence. Marginalizing Equation 23 over apparent stellar mass, we find that when all stars host the same number of planets ($Z_0 = Z_1 = Z_2$),

$$\frac{\Gamma_a(r_a)|_{r_a=r}}{\Gamma_0(r)} = \frac{1}{1+\mu} \left[1 + \frac{1}{\mathcal{N}_q} \frac{n_b}{n_s} \times \left(\int_0^1 dq\, q^\beta (1+q^\alpha)^{\frac{\gamma+4}{2}} + \right. \right.$$
$$\left. \left. \int_0^1 dq\, q^{\beta+\gamma+\frac{5}{3}} (1+q^\alpha)^{\frac{3}{2}} (1+q^{-\alpha})^{\frac{\gamma+1}{2}} \right) \right], \tag{32}$$

where ζ does not appear because of the marginalization over M_a. For $\alpha = 3.5$, $\beta = 0$, $\gamma = -2.92$, the summed integrals in Equation 32 give (...) ≈ 1.503. For $n_b/(n_b + n_s) = 0.44$, this yields $\Gamma_a/\Gamma_0 = 1.048$. The apparent rate density is 4.8% larger than the rate density around singles. Considering only twin binaries gave us good intuition: for apparent radii from $2r_\oplus$ to $17r_\oplus$, binarity influences apparent planet occurrence rates around Sun-like stars at the level of a few percent.
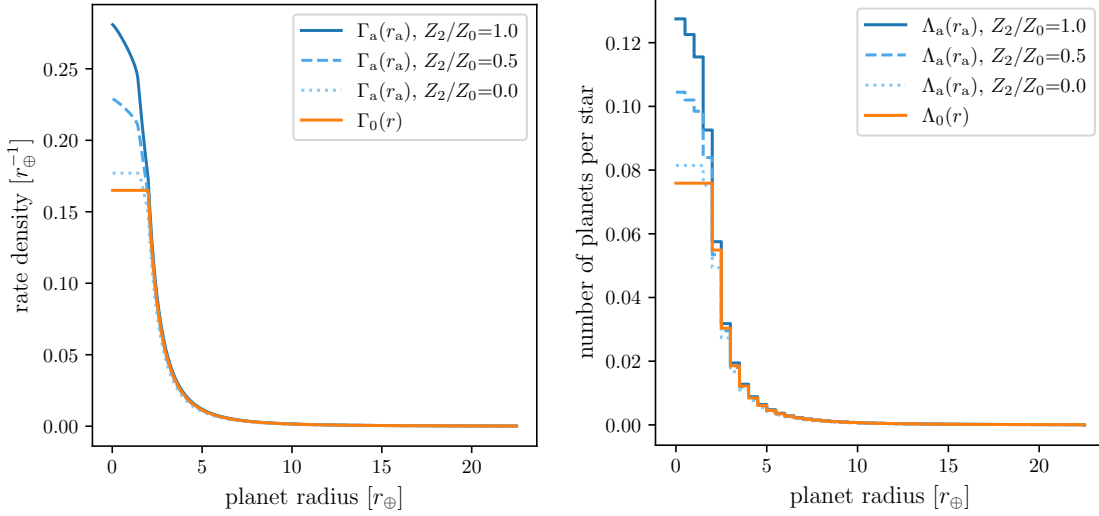
Figure 4. *Left:* apparent rate density (Γ_a) and single star rate density (Γ_0). *Right:* apparent occurrence rate (Λ_a) and single star occurrence rate (Λ_0), over $0.5 r_\oplus$ bins. The true planet radius distribution is specified by Equation 33. This model assumes that the observer knows the true properties of all the singles and primaries, and that the volume-limited mass ratios of secondaries are drawn from a uniform distribution. Further, we take $Z_0 = Z_1 = 0.5$ throughout; Z_0, Z_1, Z_2 are the number of planets per single, primary, and secondary star. The rate and rate density are related by $\Lambda|_a^b = \int_a^b \Gamma \, dr$.

5.2. *Varying stars; broken power law planet radius distribution*

Though the details of the planet radius distribution $\Gamma_i(r)$ at $r < 2r_\oplus$ are currently an active topic of research, by making plausible assumptions we can investigate how neglecting binarity might bias measurements in this regime. For instance, consider a broken power-law:

$$f(r) \propto \begin{cases} r^\gamma & \text{for } r \geq 2r_\oplus \\ \text{constant} & \text{for } r \leq 2r_\oplus. \end{cases} \tag{33}$$

At apparent radii $r_a > 2r_\oplus$, the apparent rate density in this model is the same as that in Section 5.1.2. At smaller apparaent radii the equations are tedious, but still tractable. For simplicity, we insert Equation 33 into Equation 23, and integrate using a computer program. We refer the interested reader to our online implementation[2]. As before, $L \propto M^\alpha \propto R^\alpha$, and $\alpha = 3.5$, $\beta = 0$, $\gamma = -2.92$. The output, shown in Figure 4, is validated using analytic predictions in the $r_a > 2r_\oplus$ and the $r_a < 2r_\oplus/\sqrt{2}$ regimes.

The rate of Earth analogs—The immediately arresting result is a "bump" in the apparent rate density at apparent radii below $2r_\oplus$: the true rate for singles is less than the apparent rate. If secondaries host as many planets as single stars, the occurrence

---

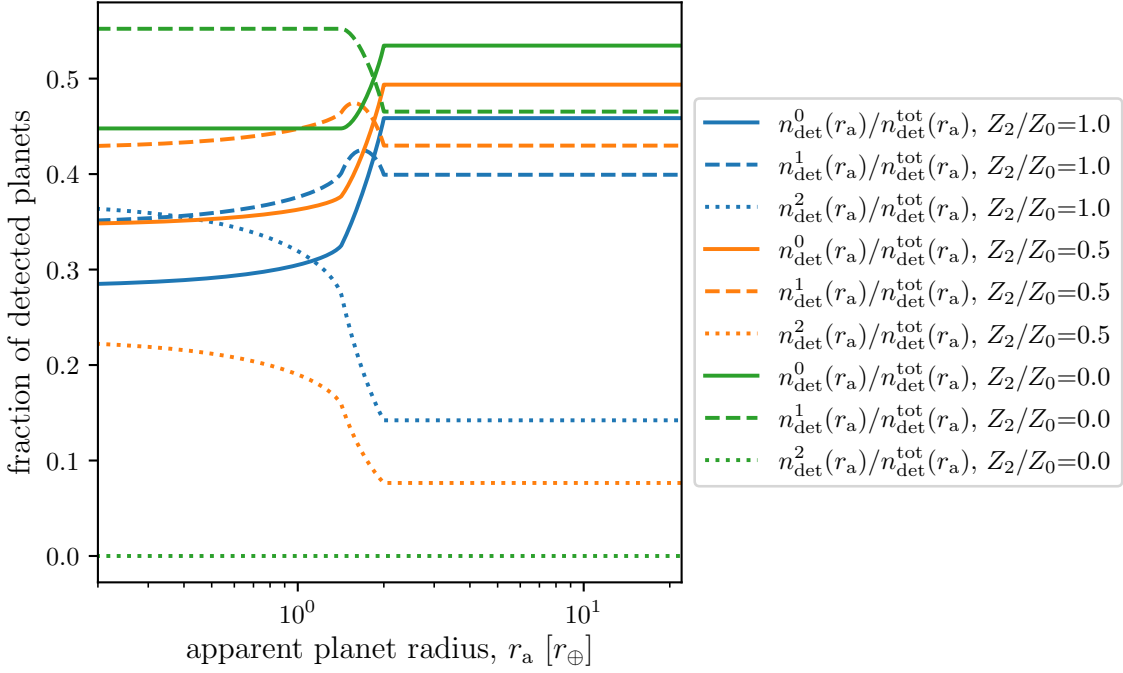[2] https://github.com/lgbouma/binary_biases

Figure 5. Fraction of detected planets at a given apparent planet radius that orbit single stars (solid lines), primaries of binaries (dashed lines), and secondaries of binaries (dotted lines). We assume that single stars and primaries have the same number of planets per star, and that the true planet radius distribution is a broken power law (same as Figure 4).

of these small planets is overestimated by $\approx 50\%$. The magnitude of the systematic error decreases if there are fewer planets around secondaries; if secondaries host no planets at all, the apparent rate is overestimated by only $\approx 10\%$.

Hot Jupiter occurrence rates—By integrating the rate density from Figure 4, we can compare the apparent hot Jupiter occurrence rate with the true rate for singles. The difference between the rates is largest when secondaries host no planets. In that case, we find $\Lambda_{\mathrm{HJ,0}}/\Lambda_{\mathrm{HJ,a}} = 1.13$, where

$$\Lambda_{\mathrm{HJ,a}} = \int_{8r_\oplus}^\infty \Gamma_a(r_a)\,\mathrm{d}r_a, \quad \text{and} \quad \Lambda_{\mathrm{HJ,0}} = \int_{8r_\oplus}^\infty \Gamma_0(r)\,\mathrm{d}r. \tag{34}$$

If secondaries host half as many planets as single stars, then $\Lambda_{\mathrm{HJ,0}}/\Lambda_{\mathrm{HJ,a}} = 1.06$. We pay further attention to the issue of hot Jupiter occurrence rates in Section 5.3.

Fraction of detected planets from a given source—A common situation during transit survey follow-up is for high-resolution imaging to reveal multiple stars in a system that shows planetary transits. It is often impossible to rule which star hosts the detected planet. Intuitively, one would expect that the primary star would be the more likely host because at fixed planet size, planetary transits around secondaries have smaller amplitudes (Equations 20 and 21 imply $\mathcal{D}_2 > \mathcal{D}_1$, if $\alpha = 3.5$). However, this reasoning is qualitative, and its assumptions might not always hold.

Our formalism lets us calculate the relative probability that a detected planet orbits a single, primary, or secondary star in a more general manner. To perform the calculation, we use expressions given in the appendix for the number of detections coming from each type of system (Equations A18, A19, and A20). We then divide out by the total number of detections at each apparent radius. Figure 5 shows the result: if high-resolution imaging reveals a source with transits to be a binary system, the detected planet does usually orbit the primary.

If the apparent radius of the system is above $2r_\oplus$, and planets exist about primaries and secondaries at equal rates, then the planet is ≈ 3 times more likely to orbit the primary than the secondary. If secondaries host half as many planets as primaries, then a detected planet is ≈ 5 times more likely to orbit the primary.

The situation for apparent radii below $2r_\oplus$ is more nuanced. For the two cases in which secondaries host fewer planets than primaries, detected planets in binaries are still always more likely to orbit the primary. However, if planets exist at the same rate in primaries and secondaries, then there is a turn-over radius, $\approx 0.4r_\oplus$, below which more of the detected planets in binaries come from secondaries – they have all been "diluted down" from larger true planetary radii! Rephrased, going from apparent radii of $2r_\oplus$ to $1.4r_\oplus$, the fraction of detected planets with binary companions increases by anywhere from 6% to 12%, depending on the relative occurrence of planets about primaries and secondaries. We compare this prediction with recent observations in Section 6.

5.3. *Further models: radius gaps, Gaussian HJ distributions*

The radius distribution specified by Equation 33 misses some important features revealed by state of the art planet occurrence studies.

Precise features of the radius valley—Fulton et al. (2017) recently reported a "gap" in the radius-period plane (Petigura et al. 2017a; Johnson et al. 2017). The existence of the gap has been independently corroborated from a sample of KOIs with asteroseismically-determined stellar parameters (Van Eylen et al. 2017). Precise measurement of the gap's features, in particular its width, depth, and shape, will require accurate occurrence rates. To illustrate binarity's role in this problem, we make identical assumptions as in Section 5.2, but instead assume an intrinsic radius distribution

$$f(r) \propto \begin{cases} r^\gamma & \text{for } r \geq 2r_\oplus, \\ 0 & \text{for } 1.5r_\oplus < r < 2r_\oplus, \\ \text{constant} & \text{for } r \leq 1.5r_\oplus. \end{cases} \tag{35}$$

Figure 6 shows the resulting true and apparent rates. If left uncorrected, binarity makes the gap appear more shallow, and flattens the step-function edges. Of course, effects unrelated to binarity would also "blur" the gap in the planet radius dimension. In particular, the valley's period-dependence is almost certainly not flat (Van Eylen
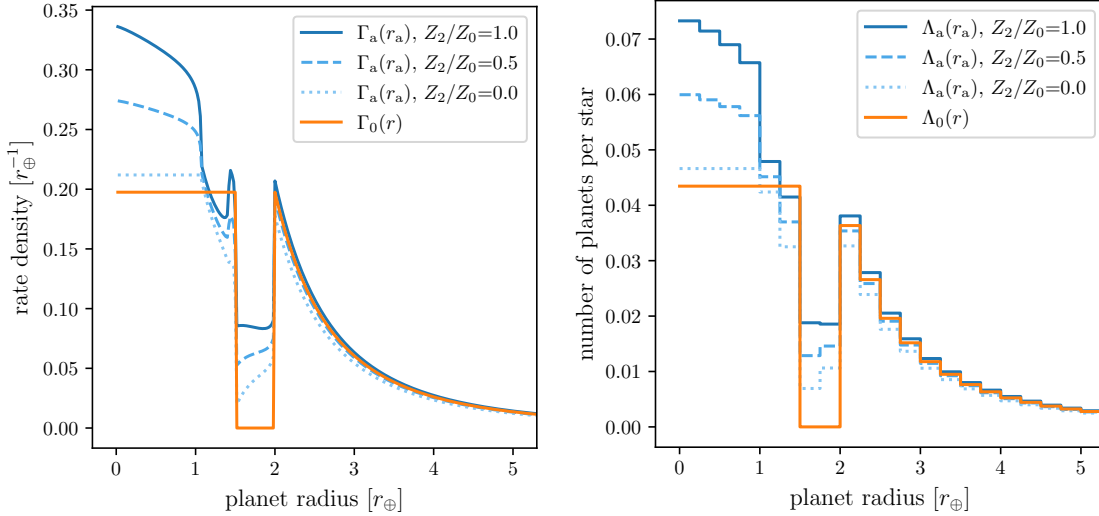
Figure 6.   *Left:* rate density and *right:* rate as a function of planet radius in a model with a radius gap (Equation 35). Other than the intrinsic radius distribution, this model has the same assumptions as Figure 4.

et al. 2017; Owen & Wu 2017). This means that any study measuring the gap's width or depth while accounting for binarity must either perform tests at fixed orbital period, or else marginalize over period and account for the associated blurring in the planet radius dimension.

The HJ distribution is not a power law—In the recent study by Petigura et al. (2017b), hot Jupiters appear as an island in period-radius space, rather than as a continuous component of a power law distribution. This means that the apparent HJ rates computed in Section 5.2 are probably inaccurate. Instead, let us consider a Gaussian radius shape function,

$$f(r) \propto \exp\left(-\frac{(r - \bar{r})^2}{2\sigma^2}\right), \tag{36}$$

with $\bar{r} = 14 r_\oplus$ and $\sigma = 2 r_\oplus$. As always, $\Gamma_i(r) = Z_i f(r)$. We then compute $\Gamma_a(r_a)$, and plot it in Figure 7. Integrating over $r_a > 8 r_\oplus$ to find hot Jupiter rates, we find the opposite effect as in the power law model. If secondaries host any planets at all, the apparent HJ rate is *greater* than the true rate for singles. For instance, if the hot Jupiter rate about secondaries and singles is equal, then $\Lambda_{HJ,0}/\Lambda_{HJ,a} = 0.81$. Qualitatively, the apparent HJ rate is greater than the true rate for singles because binary systems have extra uncounted stars that yield hot Jupiter detections.

6. DISCUSSION

How bad is ignoring binarity?—This study has shown that under a reasonable set of simplifying assumptions, ignoring binarity introduces systematic errors to star and planet counts in transit surveys, which then biases derived occurrence rates. Thus
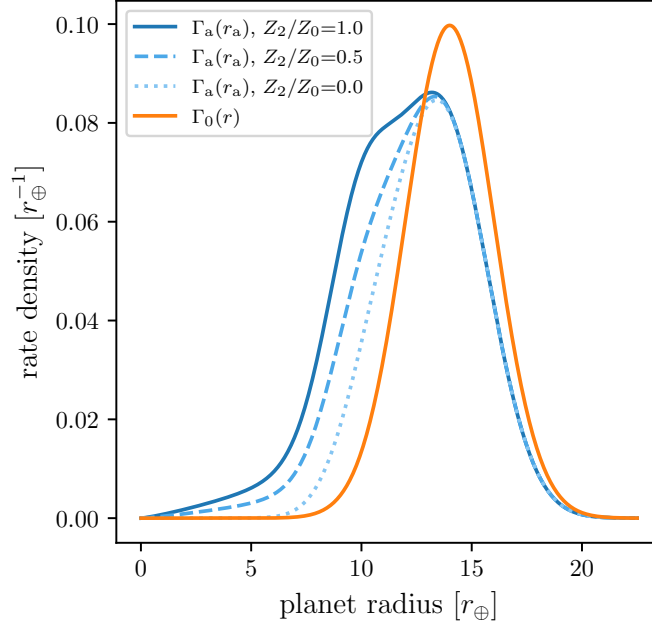
Figure 7. Rate density for a population of planets with true radii r drawn from a Gaussian with mean $14r_\oplus$ and standard deviation $2r_\oplus$. This is similar to the hot Jupiter distribution presented by Petigura et al. (2017b).

far, occurrence rate calculations[3] using transit survey data have mostly ignored stellar multiplicity (*e.g.*, Howard et al. 2012; Fressin et al. 2013; Foreman-Mackey et al. 2014; Dressing & Charbonneau 2015; Burke et al. 2015). For *Kepler* occurrence rates specifically, it seems that no one has yet carefully assessed binarity's importance, or lack thereof. This study does not resolve the problem; it only suggests the approximate scale of the systematic errors. Section 5.1 suggests that for apparent radii above $2r_\oplus$, binarity can be ignored down to a precision of a few percent. For apparent radii below $2r_\oplus$, the picture is less forgiving: Section 5.2 suggests that the apparent rates around single stars could be overestimated by as much as 50%.

The rate of Earth analogs—Youdin (2011), Petigura et al. (2013), Dong & Zhu (2013), Foreman-Mackey et al. (2014), and Burke et al. (2015) have found that between 0.03 and 1 Earth-like planets exist per Sun-like star, depending on assumptions that are made when calculating the rate (see Burke et al. 2015, Figure 17). Assuming a broken power-law, we showed that unrecognized binaries could cause overestimates in the rate of Earth analogs of up to 50%. This systematic effect is smaller than the other factors that currently dominate the dispersion in $\eta_\oplus$ measurements. If future analyses determine absolute values of $\eta_\oplus$ to better than a factor of two, binarity will likely merit closer attention.

---

[3] A list of occurrence rate papers is maintained at https://exoplanetarchive.ipac.caltech.edu/docs/occurrence_rate_papers.html

One caveat is that none of our models included the rate density's period-dependence. However, binaries with separations $\lesssim 10\,$AU could provoke dynamical instabilities, leading to fewer Earth-like planets per star (*e.g.*, Holman & Wiegert 1999; Wang et al. 2014; Kraus et al. 2016). This would affect transit survey measurements of $\eta_\oplus$ beyond our rough estimate.

Hot Jupiter rate discrepancy—While unresolved binaries may bias $\eta_\oplus$ measurements, our approach suggests that they do not influence the hot Jupiter rate discrepancy. The "discrepancy" is that hot Jupiter occurrence rates measured by transit surveys ($\approx 0.5\%$) are lower than those found by radial velocity surveys ($\approx 1\%$; see Table 1).

Though the disagreement is only weakly significant ($< 3\sigma$), one reason to expect a difference is that the RV sample is biased towards metal-rich stars, which host more giant planets (Santos et al. 2004; Fischer & Valenti 2005; Gould et al. 2006). Investigating the discrepancy from the metallicty angle, Guo et al. (2017) measured the *Kepler* field's mean metallicity to be $[\mathrm{M/H}]_{\mathrm{Kepler}} = -0.045 \pm 0.009$, which is lower than the California Planet Search's mean of $[\mathrm{M/H}]_{\mathrm{CPS}} = -0.005 \pm 0.006$. The former value agrees with that found by Dong et al. (2014). Refitting for the metallicity exponent in $\Lambda_{\mathrm{HJ}} \propto 10^{\beta[\mathrm{M/H}]}$, Guo et al. found $\beta = 2.1 \pm 0.7$, and noted that the metallicity difference could account for 0.2% of the needed 0.5% difference between the measured CKS and *Kepler* rates[4]. Guo et al. concluded that "other factors, such as binary contamination and imperfect stellar properties" must also be at play.

Radial velocity surveys usually reject visual and spectroscopic binaries (Wright et al. 2012), so their hot Jupiter rates are closer to the rate for single stars than the rates reported by transit surveys. However, we found in Section 5.3 that when assuming a Gaussian radius distribution, apparent hot Jupiter rates are *greater* than the true rate around singles: the effect goes the wrong way. There could be other systematic factors behind the difference – but they are unlikely to be related to binarity.

Does a detected planet orbit the primary or secondary?—A separate reason to address stellar multiplicity in transit surveys is that it can radically alter the interpretation of planet candidates on a system-by-system level. To identify and correct for unseen stellar companions, high-resolution imaging campaigns have surveyed almost all *Kepler* Objects of Interest (Howell et al. 2011; Adams et al. 2012, 2013; Horch et al. 2012, 2014; Lillo-Box et al. 2012, 2014; Dressing et al. 2014; Law et al. 2014; Cartier et al. 2015; Everett et al. 2015; Gilliland et al. 2015; Wang et al. 2015b,c; Baranec et al. 2016; Ziegler et al. 2017). The results of these programs have been summarized by Furlan et al. (2017), and they represent an important advance in understanding the KOI sample's multiplicity statistics.

An immediate application is to reassess the radii of detected planets. Doing so, Hirsch et al. (2017) recently found that for their sample of KOIs in binaries, the

---

[4] Petigura et al. (2017b) recently found $\beta = 3.4^{0.9}_{-0.8}$. If true, this implies that metallicity could account for about half of the "hot Jupiter rate discrepancy".

planet radii are underestimated by factors $r/r_a = 1.17$ if all planets orbit primaries, and $r/r_a = 1.65$ if detected planets are equally likely to orbit primaries and singles. This approach makes minimal assumptions about the likelihood that a planet orbits the primary vs. the secondary (though Hirsch et al. 2017 do also consider weighting radius corrections by planet occurrence).

Our approach provides a suggestion of how to assess the probability that a detected planet in a binary system orbits either component. The problem requires assuming both the underlying radius distribution, and the relative number of planets per primary and secondary star. We found that for a broken power law radius distribution, with equal occurrence rates about primaries and secondaries, detected planets in binary systems are usually more likely to orbit the primary (Figure 5). For apparent radii greater than $2r_\oplus$, the odds of primary:secondary are 8:3. The odds increase for the planet to orbit the secondary increase at smaller apparent radii, and reach 1:1 at $r_a = 0.4r_\oplus$. For *Kepler*, this suggests that for almost all confirmed KOIs in multiple star systems, the planet most likely orbits the primary.

Fraction of detected planets with binary companions—A related effect is that some detected planets are more likely to be in binary systems than others. Notably, Figure 5 predicts that the fraction of detected planets with binary companions should increase by $\approx 6 - 12\%$ going from $2r_\oplus$ to $1.4r_\oplus$.

In Ziegler et al. (2017)'s recent summary of the Robo-AO KOI survey, they reported the fraction of planet-hosting stars with Robo-AO detected companion stars, binned over apparent planet radii. The fraction of KOIs with nearby stars and their 1σ uncertainties are:

- Earths ($r_a < 1.6r_\oplus$): $16.3 \pm 1.0\%$, from 1480 systems.

- Neptunes ($1.6r_\oplus < r_a < 3.9r_\oplus$): $13.0 \pm 0.8\%$, from 2058 systems.

- Saturns ($3.9r_\oplus < r_a < 9r_\oplus$): $13.6 \pm 2.0\%$, from 338 systems.

- Jupiters ($r_a > 9r_\oplus$): $19.0 \pm 2.8\%$, from 247 systems.

The uncertainties were calculated following Burgasser et al. (2003). The absolute values of the companion fractions are lower than in the solar neighborhood at least in part because of Robo-AO's sensitivity (Ziegler et al. 2017's Figure 2; Raghavan et al. 2010). The uptick in the companion rate for Jupiters is likely tied to a large astrophysical false positive rate (Santerne et al. 2012). Going from Neptunes to Earths, the data suggest a weak increase in the detected planet companion fraction, perhaps of a few percent. It will be interesting to see whether this effect is borne out by further observations.

Connecting high-resolution imaging to occurrence rates—Occurrence rate calculations are beginning to incorporate the results of high-resolution imaging surveys. For example, recent studies have reduced contamination in the "numerator" of the occurrence rate by using Furlan et al. (2017)'s catalog to test the effects of removing KOI

hosts with known companions ([Fulton et al. 2017](); [Petigura et al. 2017b]()). This is a good first step, but the denominator remains uncorrected.

Even if the multiplicity of every star that *Kepler* surveyed were known, the problem would not be solved. In this scenario, it would be possible to tabulate planet occurrence for single and binary star systems separately. The number of planets per single star would thus be known. However the number of planets per primary and secondary would still be convolved. An observational approach to separating the two populations might be to analyze the centroids, or the transit durations (and thus host star densities) for a representative sample of planets in binary systems.

A theory-driven solution might entail probabilistic population inference, with a parametrized model for planet populations around primary and secondary stars. Such an approach might find the populations to differ, given that secondary stars are less massive, and so are perhaps more likely to host smaller planets ([Dressing & Charbonneau 2015]()). Given the difficulty of writing a correct likelihood function in a survey with systematic biases, this might only be feasible by forward-modeling the survey in the framework of approximate Bayesian computation (*e.g.*, [Morehead 2016]()).

7. CONCLUSION

This study presented a framework for estimating the impact of unresolved binaries on transit survey occurrence rates. From the order-of-magnitude argument presented in Section [3](), we showed that for Sun-like stars in the local neighborhood, typical twin binary fractions yield apparent occurrence rates that are well within a factor of two of the true rates for single stars.

We then derived a general formula for the apparent rate density inferred by observers who ignore binarity (Equation [23]()). As input, this equation requires a volume-limited mass ratio distribution, and the true rate densities for planets around singles, primaries, and secondaries. The assumptions that enable this approach are as follows.

1. The transit survey is SNR-limited (Equation [1]()).

2. The observers know the true properties of the single and primary stars, and assign all unresolved binaries the properties of the primary.

3. There are two functions, $L(M)$ and $R(M)$, that specify a star's luminosity and radius in terms of its mass.

The interpretation of Equation [23]() is that the apparent rate density is a weighted sum of the rate densities for single, primary, and secondary stars. The weights depend on the relative numbers of binary and single stars in the searchable volumes, which are affected by both dilution of transit signals and a Malmquist bias. Both effects should be considered in Monte Carlo simulations of transit surveys (*e.g.*, [Bakos et al. 2013](); [Sullivan et al. 2015](); [Günther et al. 2017]()).

Applying Equation [23](), we then showed that:

- If single, primary, and secondary stars all host the same number of planets per star, and the planet radius distribution is a power law with the exponent reported by Howard et al. (2012) at $r > 2r_\oplus$, then binarity influences apparent planet occurrence rates at the few percent level. This applies for apparent radii from $2r_\oplus$ to $17r_\oplus$ (Section 5.1).

- Assuming a broken-power law planet radius distribution, with the Howard et al. (2012) exponent above $2r_\oplus$ and a constant occurrence below $2r_\oplus$, there is a "bump" in the apparent rate density at $r_a < 2r_\oplus$. This can lead to overestimates in occurrence, $\Delta\Gamma_0 = |\Gamma_0 - \Gamma_a|/\Gamma_0$, of roughly 50% (Figure 4). Although this is smaller than current systematic uncertainties on the occurrence rates of Earth-sized planets, this implies that binarity could eventually become an important component of the $\eta_\oplus$ error budget.

- Binarity "fills in" gaps in the radius distribution (Figure 6), to a degree that could affect precise measurements of the depth, width, and slope of Fulton et al. (2017)'s radius gap, in the event that planets are not carefully vetted with high-resolution imaging.

- Binarity does not lead to smaller apparent HJ occurrence rates (Figure 7). This assumes a Gaussian planet radius distribution, similar to that reported by Petigura et al. (2017b).

- Detected planets with $r_a \gtrsim 0.5r_\oplus$ that are revealed by high-resolution imaging surveys to exist in binaries are more likely to orbit the primary (Figure 5).

- Near the "break" in occurrence rate as a function of planet radius ($\approx 2r_\oplus$), the fraction of detected planets with binary companions should increase by roughly 5 - 10% (Figure 5).

These results are only strictly applicable for idealized transit surveys meeting the criteria mentioned above. For real transit surveys, although our approach is only suggestive, we hope that it provides a rough estimate for the systematic errors that can be incurred by ignoring binarity when calculating planetary occurrence rates.

APPENDIX

A. ALTERNATIVE DERIVATION OF APPARENT RATE DENSITY

This appendix derives Equation 23 through a more straight-forward, but also more tedious, method than that presented in Section 4. First, note that analogous to Equation 2, the apparent rate density Γ_a can be written

$$\Gamma_a(r_a, M_a) = \frac{n_{\det}(r_a, M_a)}{N_\star(r_a, M_a)} \times \frac{1}{p_{\text{tra}}(M_a)}, \tag{A1}$$

where $n_{\det}$ is the number of detected planets, per unit (r_a, M_a), with apparent radius r_a orbiting stars of apparent mass M_a. The planets with (r_a, M_a) are associated with systems of many different planetary and stellar properties, so $n_{\det}(r_a, M_a)$ is given by the convolution of the true rate density, $\Gamma(r, M)$, and $\mathcal{N}_\star(r_a, M_a; r, M)$, the number of searchable stars per unit (r_a, M_a) that give (r_a, M_a) when the true system actually has properties (r, M). Mathematically,

$$n_{\det}(r_a, M_a) = \sum_i n_{\det}^i(r_a, M_a) \tag{A2}$$

$$= \sum_i \int dr dM \, \mathcal{N}_\star^i(r_a, M_a; r, M) \cdot \Gamma_i(r, M) \cdot p_{\text{tra}}(r, M), \tag{A3}$$

where i specifies the type of true host star (0: single, 1: primary, 2: secondary). The problem reduces to the evaluation of

$$\mathcal{N}_\star^i(\mathcal{P}_a, \mathcal{S}_a; \mathcal{P}, \mathcal{S}) \tag{A4}$$

for planets around single stars, primaries in binaries, and secondaries in binaries.

Single stars—For $i = 0$,

$$\mathcal{N}_\star^0(r_a, M_a; r, M) = \hat{\delta}(r_a - r)\hat{\delta}(M_a - M)N_\star^0(r, M), \tag{A5}$$

where $\hat{\delta}$ is the Dirac delta function, so

$$n_{\det}^0(r_a, M_a) = N_\star^0(r_a, M_a) \cdot \Gamma_0(r_a, M_a) \cdot p_{\text{tra}}(r_a, M_a). \tag{A6}$$

Primaries in binaries—The number of primaries with apparent parameters (r_a, M_a) given the true parameters (r, M) is

$$\mathcal{N}_\star^1(r_a, M_a; r, M) = \int dq \, f(q)\mathcal{N}_{s,q}^1(r_a, M_a, q; r, M), \tag{A7}$$

where $f(q)$ is the volume-limited binary mass ratio distribution. Since we assume that binaries are assigned the mass of the primary,

$$\mathcal{N}_{s,q}^1(r_a, M_a, q; r, M) \propto \hat{\delta}(M_a - M). \tag{A8}$$

In this case, $\mathcal{N}_{s,q}^1$ is non-zero only at $r_a = R_a\sqrt{\delta}$, and the observed depth is

$$\delta = \left[\frac{r}{R(M_a)}\right]^2 \times \frac{L(M_a)}{L_{tot}(M_a, q)} \equiv \left[\frac{r}{R(M_a)}\right]^2 \times \frac{1}{\mathcal{D}_1^2} \tag{A9}$$

where

$$\mathcal{D}_1 = \sqrt{\frac{L_{tot}(M_a, q)}{L(M_a)}}. \tag{A10}$$

The normalization of $\mathcal{N}_{s,q}^1$ is given by the number of binaries that are searchable for a signal δ and that have mass ratio q:

$$N_\star^0(\delta, L(M_a)) \cdot \frac{n_b}{n_s} \left[\frac{L_{tot}(M_a, q)}{L(M_a)}\right]^{3/2}. \tag{A11}$$

Thus,

$$\mathcal{N}_{s,q}^1(r_a, M_a, q; r, M) = N_\star^0(\delta, L(M_a)) \cdot \frac{n_b}{n_s} \cdot \mathcal{D}_1^3 \cdot \hat{\delta}\left[r_a - \frac{r}{\mathcal{D}_1}\right]\hat{\delta}(M_a - M). \tag{A12}$$

Secondaries in binaries—In this case, $M = qM_1 = qM_a$, so

$$\mathcal{N}_{s,q}^2(r_a, M_a, q; r, M) \propto \hat{\delta}\left(M_a - \frac{M}{q}\right). \tag{A13}$$

Again $\mathcal{N}_\star^2$ is non-zero only at $r_a = R_a\sqrt{\delta}$, but this time

$$\delta = \left[\frac{r}{R(qM_a)}\right]^2 \times \frac{L(qM_a)}{L_{tot}(M_a, q)} \equiv \left[\frac{r}{R(M_a)}\right]^2 \times \frac{1}{\mathcal{D}_2^2}, \tag{A14}$$

where

$$\mathcal{D}_2 = \frac{R(qM_a)}{R(M_a)}\sqrt{\frac{L_{tot}(M_a, q)}{L(qM_a)}}. \tag{A15}$$

The normalization remains the same as the previous case – we are counting the searchable stars at a given observed depth δ, and the total luminosity of the binary is the same. Thus,

$$\mathcal{N}_\star^2(r_a, M_a; r, M) = \int dq\, f(q)\mathcal{N}_{s,q}^2(r_a, M_a, q; r, M), \tag{A16}$$

where

$$\mathcal{N}_{s,q}^2(r_a, M_a, q; r, M) = N_\star^0(\delta, L(M_a)) \cdot \frac{n_b}{n_s} \cdot \mathcal{D}_1^3 \cdot \hat{\delta}\left[r_a - \frac{r}{\mathcal{D}_2}\right]\hat{\delta}\left(M_a - \frac{M}{q}\right). \tag{A17}$$

One might worry in Equation A17 that we opt to write $\mathcal{N}_s^2 \propto \hat{\delta}(M_a - M/q)$, rather than $\propto \hat{\delta}(M_a q - M)$ or some other delta function with the same functional dependence, but a different normalization once integrated. We do this because the delta function in Equation A17 is defined with respect to the measure dM_a, not dM. This is because $\mathcal{N}_s^2$ is defined as a number per r_a, per M_a.

Number of detected planets—Marginalizing per Equation A3, we find

$$
\begin{aligned}
n_{\mathrm{det}}^0(r_{\mathrm{a}}, M_{\mathrm{a}}) &= \int \mathrm{d}r \mathrm{d}M \, \mathcal{N}_\star^0(r_{\mathrm{a}}, M_{\mathrm{a}}; r, M) \cdot \Gamma_0(r, M) \cdot p_{\mathrm{tra}}(M) \\
&= N_\star^0(\delta, L(M_{\mathrm{a}})) \cdot \Gamma_0(r_{\mathrm{a}}, M_{\mathrm{a}}) \cdot p_{\mathrm{tra}}(M_{\mathrm{a}}), \quad\quad (\mathrm{A}18)
\end{aligned}
$$

and

$$
\begin{aligned}
n_{\mathrm{det}}^1(r_{\mathrm{a}}, M_{\mathrm{a}}) &= \int \mathrm{d}r \mathrm{d}M \, \mathcal{N}_\star^1(r_{\mathrm{a}}, M_{\mathrm{a}}; r, M) \cdot \Gamma_1(r, M) \cdot p_{\mathrm{tra}}(M) \\
&= N_\star^0(\delta, L(M_{\mathrm{a}})) \cdot p_{\mathrm{tra}}(M_{\mathrm{a}}) \cdot \frac{n_{\mathrm{b}}}{n_{\mathrm{s}}} \int \mathrm{d}q \, \mathcal{D}_1^3 f(q) \cdot \mathcal{D}_1 \Gamma_1(\mathcal{D}_1 r_{\mathrm{a}}, M_{\mathrm{a}}). \quad (\mathrm{A}19)
\end{aligned}
$$

Finally,

$$
\begin{aligned}
n_{\mathrm{det}}^2(r_{\mathrm{a}}, M_{\mathrm{a}}) &= \int \mathrm{d}r \mathrm{d}M \, \mathcal{N}_\star^2(r_{\mathrm{a}}, M_{\mathrm{a}}; r, M) \cdot \Gamma_2(r, M) \cdot p_{\mathrm{tra}}(M) \\
&= N_\star^0(\delta, L(M_{\mathrm{a}})) \cdot \frac{n_{\mathrm{b}}}{n_{\mathrm{s}}} + \int \mathrm{d}q \, \mathcal{D}_1^3 f(q) \cdot q \mathcal{D}_2 \Gamma_2(\mathcal{D}_2 r_{\mathrm{a}}, q M_{\mathrm{a}}) \cdot \frac{R(q M_{\mathrm{a}})}{R(M_{\mathrm{a}})} q^{-1/3}.
\end{aligned}
$$
$$(\mathrm{A}20)$$

General formula for apparent occurrence rate—Combining the above results with Equation 12, the apparent rate density,

$$
\Gamma_{\mathrm{a}}(r_{\mathrm{a}}, M_{\mathrm{a}}) = \frac{1}{N_\star(r_{\mathrm{a}}, M_{\mathrm{a}}) p_{\mathrm{tra}}(r_{\mathrm{a}}, M_{\mathrm{a}})} \times \sum_i n_{\mathrm{det}}^i(r_{\mathrm{a}}, M_{\mathrm{a}}), \quad\quad (\mathrm{A}21)
$$

evaluates to

$$
\begin{aligned}
\Gamma_{\mathrm{a}}(r_{\mathrm{a}}, M_{\mathrm{a}}) = \frac{1}{1+\mu} \cdot \Bigg\{ \Gamma_0(r_{\mathrm{a}}, M_{\mathrm{a}}) &+ \frac{n_{\mathrm{b}}}{n_{\mathrm{s}}} \Bigg[\int_0^1 \mathrm{d}q \, \mathcal{D}_1^3 f(q) \cdot \mathcal{D}_1 \Gamma_1(\mathcal{D}_1 r_{\mathrm{a}}, M_{\mathrm{a}}) \\
&+ \int_0^1 \mathrm{d}q \, \mathcal{D}_1^3 f(q) \cdot q \mathcal{D}_2 \Gamma_2(\mathcal{D}_2 r_{\mathrm{a}}, q M_{\mathrm{a}}) \cdot \frac{R(q M_{\mathrm{a}})}{R(M_{\mathrm{a}})} q^{-1/3} \Bigg] \Bigg\}.
\end{aligned}
$$
$$(\mathrm{A}22)$$

We validate this equation in limits where it is possible to write down the answer (e.g., Equation 17), and also against a Monte Carlo realization of the twin binary models (Sections 3.1 and 5.1).

Table 1. Occurrence rates of hot Jupiters (HJs) about FGK dwarfs, as measured by radial velocity and transit surveys.

Reference	HJs per thousand stars	HJ Definition
Marcy et al. (2005)	12 ± 2	$a < 0.1\,\mathrm{AU}; P \lesssim 10\,\mathrm{day}$
Cumming et al. (2008)	15 ± 6	–
Mayor et al. (2011)	8.9 ± 3.6	–
Wright et al. (2012)	12.0 ± 3.8	–
Gould et al. (2006)	$3.1^{+4.3}_{-1.8}$	$P < 5\,\mathrm{day}$
Bayliss & Sackett (2011)	10^{+27}_{-8}	$P < 10\,\mathrm{day}$
Howard et al. (2012)	4 ± 1	$P < 10\,\mathrm{day}; r_p = 8-32\,r_\oplus;$ solar subset[a]
–	5 ± 1	solar subset extended to $Kp < 16$
–	7.6 ± 1.3	solar subset extended to $r_p > 5.6\,r_\oplus$.
Moutou et al. (2013)	10 ± 3	*CoRoT* average; $P \lesssim 10\,\mathrm{day}, r_p > 4\,r_\oplus$
Petigura et al. (2017b)	$5.7^{+1.4}_{-1.2}$	$r_p = 8-24\,r_\oplus; P = 1-10\,\mathrm{day};$ CKS stars[b]
Santerne et al. (2018, in prep)	9.5 ± 2.6	*CoRoT* galactic center
–	11.2 ± 3.1	*CoRoT* anti-center

NOTE— The first four studies use data from radial velocity surveys; the rest are based on transit surveys. Many of these surveys selected different stellar samples. "–" denotes "same as above".

[a] Howard et al. (2012)'s "solar subset" was defined as *Kepler*-observed stars with $4100\,\mathrm{K} < T_{\mathrm{eff}} < 6100\,\mathrm{K}$, $Kp < 15$, $4.0 < \log g < 4.9$. They required signal to noise > 10 for planet detection.

[b] Petigura et al. (2017b)'s planet sample includes all KOIs with $Kp < 14.2$, with a statistically insignificant number of fainter stars with HZ planets and multiple transiting planets. Their stellar sample begins with Mathur et al. (2017)'s catalog of 199991 *Kepler*-observed stars. Successive cuts are: $Kp < 14.2\,\mathrm{mag}$, $T_{\mathrm{eff}} = 4700-6500\,\mathrm{K}$, and $\log g = 3.9-5.0\,\mathrm{dex}$, leaving 33020 stars.

REFERENCES

Adams, E. R., Ciardi, D. R., Dupree, A. K., et al. 2012, The Astronomical Journal, 144, 42

Adams, E. R., Dupree, A. K., Kulesa, C., & McCarthy, D. 2013, The Astronomical Journal, 146, 9

Bakos, G. ., Csubry, Z., Penev, K., et al. 2013, PASP, 125, 154

Baranec, C., Ziegler, C., Law, N. M., et al. 2016, The Astronomical Journal, 152, 18

Batalha, N. M., Borucki, W. J., Koch, D. G., et al. 2010, The Astrophysical Journal Letters, 713, L109

Bayliss, D. D. R., & Sackett, P. D. 2011, The Astrophysical Journal, 743, 103

Burgasser, A. J., Kirkpatrick, J. D., Reid, I. N., et al. 2003, The Astrophysical Journal, 586, 512

Burke, C. J., Christiansen, J. L., Mullally, F., et al. 2015, The Astrophysical Journal, 809, 8

Cartier, K. M. S., Gilliland, R. L., Wright, J. T., & Ciardi, D. R. 2015, The Astrophysical Journal, 804, 97

Christiansen, J. L., Clarke, B. D., Burke, C. J., et al. 2016, The Astrophysical Journal, 828, 99

Cumming, A., Butler, R. P., Marcy, G. W., et al. 2008, Publications of the Astronomical Society of the Pacific, 120, 531

Dong, S., & Zhu, Z. 2013, The Astrophysical Journal, 778, 53

Dong, S., Zheng, Z., Zhu, Z., et al. 2014, The Astrophysical Journal Letters, 789, L3

Dressing, C. D., Adams, E. R., Dupree, A. K., Kulesa, C., & McCarthy, D. 2014, The Astronomical Journal, 148, 78

Dressing, C. D., & Charbonneau, D. 2015, ApJ, 807, 45

Everett, M. E., Barclay, T., Ciardi, D. R., et al. 2015, The Astronomical Journal, 149, 55

Fischer, D. A., & Valenti, J. 2005, The Astrophysical Journal, 622, 1102

Foreman-Mackey, D., Hogg, D. W., & Morton, T. D. 2014, The Astrophysical Journal, 795, 64

Fressin, F., Torres, G., Charbonneau, D., et al. 2013, The Astrophysical Journal, 766, 81

Fulton, B. J., Petigura, E. A., Howard, A. W., et al. 2017, The Astronomical Journal, 154, 109

Furlan, E., Ciardi, D. R., Everett, M. E., et al. 2017, The Astronomical Journal, 153, 71

Gilliland, R. L., Cartier, K. M. S., Adams, E. R., et al. 2015, The Astronomical Journal, 149, 24

Gould, A., Dorsher, S., Gaudi, B. S., & Udalski, A. 2006, Acta Astronomica, 56, 1

Günther, M. N., Queloz, D., Demory, B.-O., & Bouchy, F. 2017, Monthly Notices of the Royal Astronomical Society, 465, 3379

Guo, X., Johnson, J. A., Mann, A. W., et al. 2017, The Astrophysical Journal, 838, 25

Hirsch, L. A., Ciardi, D. R., Howard, A. W., et al. 2017, The Astronomical Journal, 153, 117

Holman, M. J., & Wiegert, P. A. 1999, The Astronomical Journal, 117, 621

Horch, E. P., Howell, S. B., Everett, M. E., & Ciardi, D. R. 2012, The Astronomical Journal, 144, 165

—. 2014, The Astrophysical Journal, 795, 60

Howard, A. W., Marcy, G. W., Bryson, S. T., et al. 2012, The Astrophysical Journal Supplement Series, 201, 15

Howell, S. B., Everett, M. E., Sherry, W., Horch, E., & Ciardi, D. R. 2011, The Astronomical Journal, 142, 19

Hunter, J. D. 2007, Computing in Science & Engineering, 9, 90

Jenkins, J. M., Caldwell, D. A., & Borucki, W. J. 2002, The Astrophysical Journal, 564, 495

Johnson, J. A., Petigura, E. A., Fulton, B. J., et al. 2017, arXiv:1703.10402 [astro-ph]

Jones, E., Oliphant, T., Peterson, P., et al. 2001, Open source scientific tools for Python

Kraus, A. L., Ireland, M. J., Huber, D., Mann, A. W., & Dupuy, T. J. 2016, The Astronomical Journal, 152, 8

Law, N. M., Morton, T., Baranec, C., et al. 2014, The Astrophysical Journal, 791, 35

Lillo-Box, J., Barrado, D., & Bouy, H. 2012, Astronomy and Astrophysics, 546, A10

—. 2014, Astronomy and Astrophysics, 566, A103

Marcy, G., Butler, R. P., Fischer, D., et al. 2005, Progress of Theoretical Physics Supplement, 158, 24

Mathur, S., Huber, D., Batalha, N. M., et al. 2017, The Astrophysical Journal Supplement Series, 229, 30

Mayor, M., Marmier, M., Lovis, C., et al. 2011, ArXiv e-prints, 1109, arXiv:1109.2497

McKinney, W. 2010, in Proceedings of the 9th Python in Science Conference, ed. S. van der Walt & J. Millman, 51

Morehead, R. C. 2016, Ph.D. Thesis

Moutou, C., Deleuil, M., Guillot, T., et al. 2013, Icarus, 226, 1625

Owen, J. E., & Wu, Y. 2017, arXiv:1705.10810 [astro-ph]

Pepper, J., & Gaudi, B. S. 2005, The Astrophysical Journal, 631, 581

Pepper, J., Gould, A., & Depoy, D. L. 2003, Acta Astronomica, 53, 213

Petigura, E. A., Howard, A. W., & Marcy, G. W. 2013, Proceedings of the National Academy of Science, 110, 19273

Petigura, E. A., Howard, A. W., Marcy, G. W., et al. 2017a, arXiv:1703.10400 [astro-ph]

Petigura, E. A., Marcy, G. W., Winn, J. N., et al. 2017b, arXiv:1712.04042 [astro-ph]

Raghavan, D., McAlister, H. A., Henry, T. J., et al. 2010, The Astrophysical Journal Supplement Series, 190, 1

Santerne, A., Daz, R. F., Moutou, C., et al. 2012, Astronomy and Astrophysics, 545, A76

Santos, N. C., Israelian, G., & Mayor, M. 2004, Astronomy and Astrophysics, 415, 1153

Sullivan, P. W., Winn, J. N., Berta-Thompson, Z. K., et al. 2015, The Astrophysical Journal, 809, 77

Van Eylen, V., Agentoft, C., Lundkvist, M. S., et al. 2017, arXiv:1710.05398 [astro-ph]

Walt, S. v. d., Colbert, S. C., & Varoquaux, G. 2011, Computing in Science & Engineering, 13, 22

Wang, J., Fischer, D. A., Horch, E. P., & Huang, X. 2015a, The Astrophysical Journal, 799, 229

Wang, J., Fischer, D. A., Horch, E. P., & Xie, J.-W. 2015b, The Astrophysical Journal, 806, 248

Wang, J., Fischer, D. A., Xie, J.-W., & Ciardi, D. R. 2015c, The Astrophysical Journal, 813, 130

Wang, J., Xie, J.-W., Barclay, T., & Fischer, D. A. 2014, The Astrophysical Journal, 783, 4

Wright, J. T., Marcy, G. W., Howard, A. W., et al. 2012, The Astrophysical Journal, 753, 160

Youdin, A. N. 2011, ApJ, 742, 38

Ziegler, C., Law, N. M., Baranec, C., et al. 2017, arXiv:1712.04454 [astro-ph]